

Modeling micro-heterogeneity in mixtures: the role of many body correlations

Anthony Baptista and Aurélien Perera

Laboratoire de Physique Théorique de la Matière Condensée (UMR CNRS 7600), Sorbonne Université, 4 Place Jussieu, F75252, Paris cedex 05, France.

Abstract

A two-component interaction model is introduced herein, which allows to describe macroscopic miscibility with various modes of tunable micro-segregation, ranging from phase separation to micro-segregation, and in excellent agreement for structural quantities obtained from simulations and the liquid state hypernetted-chain like integral equation theory. The model is based on the conjecture that the many-body correlation bridge function term in the closure relation can be divided into one part representing the segregation effects, which are modeled herein, and the usual part representing random many body fluctuations. Furthermore, the model allows to fully neglect these second contributions, thus increasing the agreement between the simulations and the theory. The analysis of the retained part of the many body correlations gives important clues about how to model the many body bridge functions for more realistic systems exhibiting micro-segregation, such as aqueous mixtures.

1 Introduction

One of the central problem in statistical mechanics of liquids and mixtures is to understand both qualitatively and quantitatively the role of many-body effects on pair correlations[1, 2]. In its current state of development and application, liquid state integral equation theory (IET) is mostly a theory formulated in terms of pair interactions and pair correlations[1, 2, 3] , even though higher order correlations are incorporated implicitly by the formalism

itself and explicitly through the so-called bridge term. Neglecting this term or using approximations involving only pair correlations, leads to the usual strategies to generate approximate IET[1, 2, 3]. By comparing pair correlations obtained from such approximate IET to those obtained from computer simulations, one generally finds a rather good agreement for various types of simple liquids[4], which in turn suggests that the contribution from explicit many body correlations remains quantitatively small, although being qualitatively important. This agreement breaks down in the vicinity of phase transition, such as the gas-liquid phase separation for one component liquids, or demixing transitions for mixtures. This breakdown is intuitively understood from the paramount importance of fluctuations through the Renormalisation Group theory approach for liquids[5, 6], indicating that many body correlations become essential in such cases, although they globally remain quantitatively small[6]. Interestingly, approximate IET also break down when considering realistic liquids which exhibit micro-structure[7]. Such liquids, which we call complex liquids, encompass associating liquids, such as water and other hydrogen bonding liquids, and mixtures which show micro-segregation, the latter for which it is often impossible to solve IET[7, 8].

From these observations it is tempting to postulate that the breakdown of approximate IET is always caused by special types of spatial fluctuations, such as critical ones or those related to spatial heterogeneity, which reflects the importance of very specific types of many body correlations, and which cannot be described by the usual approximations for IET. To be more specific, approximate IET may be able to solve for micro-segregated systems, but not with the required accuracy or quite simply fail beyond a certain point, precisely because very specific forms of the many-body contributions are required. It is these specific contributions, we propose to consider as an effective interaction. Remaining correlations are considered as contributions from random fluctuations, whose importance is similar to those in simple liquids, and therefore can be neglected in approximate integral equation methods, since the principal many body effects from non-random fluctuations are already captured through the effective interactions.

The method of choice to investigate this approach is the hyper-netted chain (HNC) approximation, which precisely consists in neglecting contributions from high order correlation through the bridge term[9, 10, 11]. Interestingly, HNC is well known for having spurious tendency to fail for the type of complex liquids mentioned above, which lesser approximate IET do not have, although these do not necessarily provide solutions in agreement with the expected ones[12, 13]. This failure is the starting point for the proposal in this work, which consists in conjecturing that this shortcoming of HNC is the signature that particular forms of the bridge function are required to

describe such systems.

Assuming these assumptions holds, it remain to find which particular form of the bridge functions are required. Searching for clues, we first note that HNC can handle fluctuations in several typical cases. The first case concerns simple liquids and mixtures, such as Lennard-Jonesiums or weakly polar liquids, for which there is no particular local order. For such systems, the HNC approximation is fairly good[4], and it is for this type of systems that more accurate alternative empirical approximations have been developed, such as the Verlet bridge[14] and many other methods[4, 15, 16, 17]. The second case concerns classes of liquids which present a strong local order which dominates the typical disorder of the liquid state. One such example concerns ionic melts, such a molten NaCl for example, which are characterised by charge order[18, 19, 20, 21], where positive and negative charges are disposed in quasi-alternate fashion. HNC is often found to describe the structure of such liquids very accurately, even to extremely high couplings[22]. With these two considerations in mind, we note that all micro-segregating systems are governed by strong Coulomb interactions, and it is precisely these interactions that produce the segregation[30]. Therefore, if HNC is very good for some Coulomb systems and not for others, it means that the bridge function of the latter systems must have a very specific form and role, confirming the ideas developped above. Another example concerns the so-called core-softened interactions[23, 24, 25], which aim to describe particular forms of local order, such as that found in globular clustering[23] or in water[24]. Among this category, the repulsive core-softened interaction is particularly well described by the HNC approximation and in excellent agreement with simulations, both for pattern formations[26] or water-like models[27]. Since these models concerns non-ionic systems, They give an indirect clue about the type of pseudo-interactions which could mimic local order similar to that induced by Coulomb interactions, without having to explicitly take them into account. This can be achieved through the closure relation, as shown in the next section.

In this work, we wish to test these ideas through simple isotropic pair interactions, but which contain the bridge part which concerns the formation of micro-structure. If we formulate properly the effective pair interactions, that is the concerned bridge part, we should able to describe the whole expected scenario of micro-structure, as seen from various experimental conditions. In addition, a proper formulation should allow to neglect contributions from random fluctuations, and in such case the HNC approximation should be highly reliable. The several cases we wish to model concern the type of micro-segregation found in aqueous mixtures. For example, aqueous mixtures of small amphiphile molecules such as alcohols, are known to produce

micro-segregation[28, 29, 30], which induces large pre-peaks in atom-atom structure factors[30]. IET are generally unable to provide solutions for such mixtures (as in water-1propanol) [31], or when they can, the description of the structure is very poor (as in water-methanol)[7]. In addition to the pre-peak witnessing domain-domain correlations, the $k = 0$ behaviour of the structure factor is equally critical. For example, a large value would indicate large domain fluctuations, and not necessarily an underlying phase separation. These examples further support the idea that micro-heterogeneity is a different form of fluctuation than those which control phase transitions.

In the next section, we reformulate the conjecture in a more formal way, and we explain the modeling and computational details. In section III, we show the results of various modeling strategies, which allow to extract key features of the effective interactions. In the last section, we will discuss how these results can be extended to more realistic case, before we conclude.

2 Theoretical and computational details

2.1 From many body correlations to effective interactions

To be more specific about the statements of the Introduction, let us consider the most general form[3, 4] of the pair distribution function $g_{ab}(r)$ for a mixture of atomic sites, interacting through spherically symmetric pair interaction $v_{ab}(r)$:

$$g_{ab}(r) = \exp(-\beta v_{ab}(r) + h_{ab}(r) - c_{ab}(r) + b_{ab}(r)) \quad (1)$$

where the index a and b designate atomic species in the mixture, $h_{ab}(r) = g_{ab}(r) - 1$, $c_{ab}(r)$ is the pair direct correlation function, and $\beta = 1/k_B T$ is the Boltzmann factor (with k_B the Boltzmann constant and T the temperature). The last function $b_{ab}(r)$ is the so-called bridge function[9, 11] which contains all the many body higher order correlations, namely through the introduction of n -body direct correlation functions $c_{a_1 a_2 \dots a_n}^{(n)}(\vec{r}_1, \vec{r}_2, \dots, \vec{r}_n)$, where the index a_i is a species index, (n) designating the rank or order of correlations and \vec{r}_i designating the position of particle i of species a_i :

$$b_{ab}(r) = \sum_{m \geq 3} \frac{1}{m!} b_{ab}^{(m)}(r) \quad (2)$$

with

$$b_{ab}^{(m)}(r) = \sum_{k \geq 3} \frac{1}{k!} \sum_{s_1 \dots s_k} \left(\prod_{l=1}^k \rho_{s_l} \right) T_{ab s_1 \dots s_k}^{(k)}(r) \quad (3)$$

and

$$T_{ab s_1 \dots s_k}^{(k)}(r) = \int d\vec{r}_{13} \int d\vec{r}_{14} \dots \int d\vec{r}_{1k} \left(\prod_{l=1}^k h_{as_k}(r_{1k}) \right) c_{bs_1 \dots s_n}^{(k+1)}(\vec{r}_2, \vec{r}_3, \dots, \vec{r}_k) \quad (4)$$

where we have used the isotropy and translational invariance in macroscopically homogeneous liquid mixtures, with $r = |\vec{r}_{12}|$, $r_{ij} = |\vec{r}_{ij}| = |\vec{r}_j - \vec{r}_i|$. This simplification has been omitted in the argument of the n-body direct correlation function, in order to avoid explicitly counting all combinations of r_{ij} , but it is obviously implied.

There is a striking complexity level difference between Eq.(1) and those defining $b_{ab}(r)$. Tentative to compute low order contributions to $b_{ab}(r)$, either through Mayer bond[10] or directly from Eqs.(2-4) by approximating the function $c^{(3)}$ [32], have indicated that the density expansion is diverging. This has been directly confirmed by the exact computation of series expansion for the case of 1-dimensional hard sphere fluid. It is therefore hopeless to evaluate $b_{ab}(r)$ term by term, and one should model this term directly by some general guiding rules. This is what approaches such as the Verlet bridge[14] and all its descendants[4, 15, 16, 17] have tried to do. In the present work, we propose a different route, based on the existence of the two categories of local order described in the Introduction.

The conjecture formulated in the Introduction can be written as:

$$b_{ab}(r) = b_{ab}^{(LF)}(r) + b_{ab}^{(RF)}(r) \quad (5)$$

where $b_{ab}^{(LF)}(r)$ corresponds to many-body contributions to the local fluctuations (LF), while $b_{ab}^{(RF)}(r)$ corresponds to random fluctuations (RF). For simple liquids one has

$$b_{ab}(r) \approx b_{ab}^{(RF)}(r) \quad \text{simple liquids} \quad (6)$$

and it is this term that are usually approximated in methods designated to improve IET.

The lowest approximation level in the diagrammatic expansion in $b_{ab}(r)$ consist in setting $b_{ab}(r) = 0$, which is known as the hypernetted-chain approximation (HNC)

$$g_{ab}(r) = \exp(-\beta v_{ab}(r) + h_{ab}(r) - c_{ab}(r)) \quad (7)$$

Other levels of approximation involved further manipulation of the HNC closure (such as the PY or MSA approximations[3]), or adhoc functional

expression for $b_{ab}(r)$ which are based on various empirical basis (such as the Verlet approximation and the large number of variants based on it). Since the HNC closure represents the lowest approximation level based on the rigorous developments, we will exclusively consider this approximation below, deliberating neglecting various other approximations which are sometimes considered as more accurate from various types of empirical considerations.

In cases where complex local order is present, that is when particles tend to form local patterns (such as chaining in the case of dipolar molecules[33], for example), we postulate that the influence of the $b_{ab}^{(LF)}(r)$ term cannot be neglected, and, therefore, the HNC approximation is inappropriate. This is true in particular for aqueous mixtures which exhibit micro-segregation. In order to account for such local order, one must guess a functional form for the $b_{ab}^{(LF)}(r)$ term, while the $b_{ab}^{(RF)}(r)$ term can be neglected in a first approximation. We postulate that $b_{ab}^{(LF)}(r)$ must have generic functional forms, and can be modeled properly if such forms are known. With this idea in mind, the new form of the HNC approximation can be rewritten as

$$g_{ab}(r) = \exp(-\beta\tilde{v}_{ab}(r) + h_{ab}(r) - c_{ab}(r)) \quad (8)$$

where

$$\beta\tilde{v}_{ab}(r) = \beta v_{ab}(r) - b_{ab}^{(LF)}(r) \quad (9)$$

represents the effective interaction which accounts for the local order. One justification for this rewriting is the success of some core-soft models, for which we consider that the second outer core is in fact a representation of $-b_{ab}^{(LF)}(r)$. Another class of models which justify the rewriting concerns the so-called SALR 1-component models[2, 3, 4, 5] (SALR stands for short range attraction, long range repulsion), where the long range repulsion part accounts for the $-b_{ab}^{(LF)}(r)$ and which helps stabilize the local clustering in these models.

2.2 From effective interactions to the $b^{(LF)}(r)$ bridge function

In this part, we propose to determine the $b_{ab}^{(LF)}(r)$ term by using pseudo-potentials instead of the original interactions which produce the micro-segregation and the relevant complex disorder. In order to do that, we first observe that complex disorder is invariably produced by strong orientational interactions, and more particularly hydrogen bonding interactions for the cases we are concerned with. In the classical force field approach, hydrogen bonding is described through Coulomb pairing interactions and partial charges z_a on

selected atomic sites a , such as oxygen, hydrogen and nitrogen atoms, for example. Typical classical force field used in computer simulation of molecular liquids are of the form:

$$v_{ab}(r) = v_{ab}^{(LJ)}(r) + v_{ab}^{(C)}(r) \quad (10)$$

where $v^{(LJ)}(r) = 4\epsilon_{ab} \left[(\sigma_{ab}/r)^{12} - (\sigma_{ab}/r)^6 \right]$ is the standard (12-6) Lennard-Jones pair interaction, and $v_{ab}^{(C)}(r) = z_a z_b e^2 / r$ is the Coulomb pair interaction.

From the statistical theory of liquids, it is well known that the pair direct correlation functions is related to the pair interaction $v_{ab}(r)$ at large separations, through the exact relation[3]:

$$\lim_{r \rightarrow \infty} c_{ab}(r) = -\beta v_{ab}(r) \quad (11)$$

This relation is used to handle numerically the long range part of the Coulomb interaction $v_{ab}^{(C)}(r)$ in a convenient way[22], by separating out the short range part $c_{ab}^{(SR)}(r)$ of $c_{ab}(r)$ from a long range part which is handled analytically through an error function[22]:

$$c_{ab}(r) = c_{ab}^{(SR)}(r) - A_{ab} \frac{\text{erf}(\alpha_{ab} r)}{r} \quad (12)$$

where $A_{ab} = -z_a z_b \beta e^2$ (where z_i is the valence of atom i and e is the elementary charge), and α_{ab} is chosen such that it is smaller than the particle diameter σ_{ab} . This latter point is very important since it means that, for distances larger than α_{ab} , $r > \alpha_{ab}$, the error function part of $c_{ab}(r)$ in Eq.(12) exactly cancels the corresponding Coulomb interaction $v_{ab}^{(C)}(r)$ in the closure relation Eq.(1). This implies that the closure equation can be exactly rewritten as:

$$g_{ab}(r) = \exp \left(-\beta v_{ab}^{(LJ)}(r) + h_{ab}(r) - c_{ab}^{(SR)}(r) + b_{ab}(r) \right) \quad (13)$$

where only the short range interactions remain. While this might be a useful trick[22], the closure in Eq.(13) is rigorously equivalent to Eq.(1) for distances outside particles overlap such that $g_{ab}(r) \neq 0$. Eq.(13) is very interesting in our case because it allows to understand the role played by the bridge term $b_{ab}(r)$. Indeed, if we consider a system interacting solely through LJ type interactions, then Eq.(13) indicates that, whatever the features attesting the existence of micro-segregation in the pair correlation functions $g_{ab}(r)$, $h_{ab}(r)$ and $c_{ab}^{(SR)}(r)$, these features can arise only through the term $b_{ab}(r)$, which now plays the role of an supplementary pseudo potential. If we remove this term,

then we are back to simple disordered LJ liquids where no micro-segregation or clustering can appear. Eq.(13) is the formal proof that one could consider pair distribution functions $g_{ab}(r)$ taken from a micro-segregated system and find $b_{ab}(r)$ which will produce the same pair correlations for the effective interaction $\tilde{v}_{ab}(r) = v_{ab}^{(LJ)}(r) - b_{ab}(r)/k_B T$, now defined in terms of the non-Coulomb part of the pair interaction. Conversely, if the appropriate $b_{ab}(r)$ are injected as pseudo-interactions in an ordinary LJ mixture, it will turn it into a micro-segregating mixture, with the same pair distribution functions $g_{ab}(r)$. In this perspective, Eq.(13) now becomes a strict HNC closure, which can be solved in conjunction with the Ornstein-Zernike (OZ) equation[3] for the pseudo-system. Obviously, the corresponding direct correlation $c_{ab}(r)$ will differ from the solution of the original system, since it does not obey the same OZ equation which involves the full Coulomb interactions.

We can use the above equivalence to our advantage to extract the $b_{ab}^{(LF)}(r)$ term which we seek. We can use toy interactions which produce clustering and micro-segregation in a model mixture, which produces pair distribution functions $g_{ab}(r)$ similar to those found in realistic mixtures, and we can solve HNC for such models and see how well we reproduce the desired features in $g_{ab}(r)$. The pseudo potential is supposed to contain a standard repulsion-attraction part $v_{ab}^{(0)}(r)$, which handles the core and the dispersive parts of the interactions, and a supplementary part $v_{ab}^{(S)}(r)$ which accounts for the complexity (clustering, micro-segregation):

$$\tilde{v}_{ab}(r) = v_{ab}^{(0)}(r) + v_{ab}^{(S)}(r) \quad (14)$$

The results above suggest that $b_{ab}(r) = -\beta v_{ab}^{(S)}(r)$ is the bridge term we seek. In practice however, the HNC solution for the pseudo-system may not exactly match that of the simulated pseudo-system, because of the bridge term related to the pseudo-system itself. The key assumption of this paper is that the most appropriate analytical form of pseudo-potential $v_{ab}^{(S)}(r)$ would match the local fluctuation part of the bridge function $b_{ab}^{(LF)}(r)$ introduced in Eq.(5), even though it may not match the full bridge function. The differences between the $g_{ab}(r)$ obtained from HNC and the real model system would then be attributable to either incorrect modeling of the pseudo-potential $v_{ab}^{(S)}(r)$, or to the physical importance of the random fluctuation part of the bridge function $b_{ab}^{(RF)}(r)$ in Eqs.(5,6). This can be tested only through trial and error, as shown in the Results section.

We can now reformulate the expression for the bridge function we seek as:

$$b_{ab}^{(LF)}(r) = -\beta v_{ab}^{(S)}(r) \quad (15)$$

which, together with Eq.(14) is the principal result of this paper.

Summarising our strategy, instead of considering the full model, which creates a specific form of local order, we mimic such system by projecting the many-body $-b_{ab}^{(LF)}(r)$ term into the effective interaction. This way, using the HNC approximation in Eq.(8), we freeze the local ordering by imposing it directly into the pair interactions, and expect that we can neglect the contributions of the random fluctuations by setting $b_{ab}^{(RF)}(r) = 0$. It is important to realise that, when adopting this attitude, the usual control parameters such as the temperature and the density do not have the same meaning. Indeed, the effective interaction term $-b_{ab}^{(LF)}(r)$ is supposed to depend on such parameters, and change when these are varied. Instead, one should *adapt* newer forms of the full effective interaction $\tilde{v}_{ab}(r)$ to the expected local order which depends on different temperatures and densities.

2.3 Structure factors

We monitor the desired forms of order by looking at their manifestations in the pair correlation functions $g_{ab}(r)$ as well as in the corresponding structure factors $S_{ab}(k)$

$$S_{ab}(k) = \delta_{ab} + \rho \sqrt{x_a x_b} \int d\vec{r} [g_{ab}(r) - 1] \quad (16)$$

We emphasize that, at this stage of the exploration, it is not essential to compute thermo-physical properties, nor to expect that these would agree well with the expected values (as obtained from computed from simulations, for example). Indeed, these would still depend on the magnitude of the neglected $b_{ab}^{(RF)}(r)$ terms. For these reasons, we will focus solely on comparing $g_{ab}(r)$ and $S_{ab}(k)$ with the corresponding values computed through the computer simulations. Furthermore, in order to appreciate the relation between local order and $b_{ab}^{(LF)}(r)$, we will try as much as possible to minimize the $b_{ab}^{(RF)}(r)$. In other words, we wish to model $\tilde{v}_{ab}(r)$ in such a way that the HNC approximation is quasi-exact for the corresponding model system. In this way, we expect to find universal forms of the bridge functions with account for the micro-segregation in more realistic models. Indeed, it is important to note that the present formulation considers atomic sites, but does not specify if these belong to molecules or not. For example, in the site-site formulation of molecular liquids[34], the closure relation Eq.(1) does not contain any reference to the molecular nature. It is only at the level of the Ornstein-Zernike (OZ) equation that the molecular shape is introduced, for example through the W-matrix in the site-site OZ equation[34, 1]. From this point of view, the present formulation is perfectly general, and should be able to describe

molecular liquids as well, and in particular associating hydrogen bonding liquids.

In addition to the structure factors in Eq.(16), which represent species-species density correlations $S_{ab}(k) = \langle \rho_{a;\mathbf{k}} \rho_{b;-\mathbf{k}} \rangle$, where $\rho_{c;\mathbf{k}}$ is the Fourier transform of the instantaneous microscopic density of species c , we monitor the so-called Bathia-Thornton (BT) structure factors[6] which represent the correlations between total microscopic density $\rho_{N;\mathbf{k}} = \rho_{1;\mathbf{k}} + \rho_{2;\mathbf{k}}$ and “concentration” density $\rho_{C;\mathbf{k}} = x_2 \rho_{1;\mathbf{k}} - x_1 \rho_{2;\mathbf{k}}$. The resulting BT structure factors are related to the previous structure factors, the most interesting relations being:

$$S_{NN}(k) = \frac{1}{2} [S_{11}(k) + S_{22}(k)] + S_{12}(k) \quad (17)$$

$$S_{CC}(k) = x_2^2 S_{11}(k) + x_1^2 S_{22}(k) - 2x_1 x_2 S_{12}(k) \quad (18)$$

These structure factors are helpful in the way they allow the interpret k -dependent fluctuations in terms of global density variables instead of species related variables, hence reflecting the global heterogeneity of the system. $S_{NN}(k)$ is the equivalent of an effective 1-component structure factor for the mixture, while $S_{CC}(k)$ reflects the relative heterogeneity between the 2 components. This way, the BT representation allows to separate the homogeneous and heterogeneous components from the $S_{ab}(k)$ structure factors.

2.4 Models of the effective interactions

As stated in the Introduction, micro-heterogeneity in realistic systems is produced principally through Coulomb interactions, which tend to create a strong local order, which necessitates explicit contributions from high order correlations. In this work, we do not wish to address directly the problem by explicitly taking into account Coulomb interactions. Yet, we would like to capture the corresponding local heterogeneity. To be more precise, we would like to capture the specific heterogeneity which cannot be addressed by HNC in the realistic case. The central idea is to consider that the realistic system itself introduces the specific many-body correlations, in addition to the realistic interactions that creates the micro-heterogeneity. This is somewhat similar to going from the atomic representation of a molecule to the molecular representation as an aggregate of atoms. The specific bridge term $b^{(LF)}(r)$ are considered here to play the role of an “intra-aggregate” interaction. This way, we intend to reduce the initial problem to that of considering only this reduced interaction.

In order to model such pseudo-interactions, we rely on previous investigations, such as the SALR interactions mentioned previously, which are known to produce micro-segregation effects. In addition, we search for other similar forms, but with the idea in mind that HNC should be sufficient to describe the system, in other words $b^{(RF)}(r) \approx 0$. This way, we can compare the results of HNC with those of computer simulations of systems with substituted interactions, in place of the realistic ones. The task of testing the forms of the $b_{ab}^{(LF)}(r)$ for different types of realistic interactions showing micro-segregation, is relegated to subsequent investigations.

The SALR one-component model, mentioned above, consists of the usual short range repulsion and a long range attraction, both of which ensuring a condensed liquid phase, followed by a weak long range repulsion, which controls the formation of local aggregation in restricted parts of the phase diagram. Such types of models have been intensely investigated in the past[2, 3, 4, 5]. The standard SALR model contains 2 exponential in order to model the short range attraction and the long range repulsion, and has the same form as Eq(14):

$$\tilde{v}(r) = v_0(r) - \epsilon_1 \sigma \frac{\exp[-(r - \sigma)/\kappa_1]}{r} + \epsilon_2 \sigma \frac{\exp[-(r - \sigma)/\kappa_2]}{r} \quad (19)$$

where $v_0(r)$ is a bare interaction terms, which takes into account the particle core and any dispersive interaction. This could be a Lennard-Jones (LJ) interaction, or a soft sphere $1/r^{12}$ interaction. In the remaining two other contributions, all the ϵ_α parameters are positive and have the dimension of an energy, and σ is the diameter of the particle. The first Yukawa interaction helps aggregate particles, while the second Yukawa helps segregate the aggregates formed by the first. Unfortunately, the one-component model neglects the crucial role of the solvent in the auto-organisation process which enforces the aggregation of the solute. For example, this is one of the essential feature behind the hydrophobic effect[25] .

In the present work, we propose to extend this model to a 2 component system, which consists in of both mono-atomic solvent, labeled 1, and a solute, labelled 2, interacting through the usual short range repulsion. We will consider only models where both the solvent and the solute have the same size with a common diameter $\sigma_{11} = \sigma_{22} = \sigma$. The cross diameter σ_{12} was initially left free, as to consider non-additivity, but the final retained choice was also $\sigma_{12} = \sigma$. Tests for $\sigma_{22} > \sigma_{11}$ did not alter the main conclusion of this work as far as the working hypothesis behind Eq.(5) is concerned, and will be reported elsewhere. The key feature is in the cross-interaction modeling. The interactions are as follows

$$\tilde{v}_{11}(r) = \tilde{v}_{22}(r) = v_0(r) \quad (20)$$

$$\tilde{v}_{12}(r) = v_{12}^{(0)}(r) + v_{12}^{(\text{rep})}(r) + v_{12}^{(\text{att})}(r) \quad (21)$$

The cross-species interaction $\tilde{v}_{12}(r)$ contains, in addition to the $v_{12}^{(0)}(r)$ term, two additional contribution, the first $v_{12}^{(\text{rep})}(r)$ which repel particles of different species, hence leading to macroscopic demixion, and the second $v_{12}^{(\text{att})}(r)$ which controls this demixing tendency, leading to micro-segregation. This is very different from the SALR model, since it is exactly the opposite tendency. We propose to call this new model SRLA, by analogy with SALR. An alternate model to SRLA would have been to implement the SALR mechanism for the solvent and the solute separately, leaving the cross interaction neutral. However, this would require more adjustable parameters, with no clear justification as how one would choose to control the relative balance between repulsion and attraction for each of the components. The SRLA model is the minimal model for the purpose defined herein.

The desired bridge function $b_{12}^{(LF)}(r)$ is then given by Eq.(15):

$$b_{12}^{(LF)}(r) = -\beta v_{12}^{(\text{rep})}(r) - \beta v_{12}^{(\text{att})}(r) \quad (22)$$

while the like-bridge terms are set to zero: $b_{11}^{(LF)} = b_{22}^{(LF)} = 0$, since in the present formulation, the micro-segregation is supported only by the cross interactions.

2.5 Integral equation theory

This theory consists in solving the Ornstein-Zernike and a closure equation, for which we use here the HNC closure of Eq.(8), in order to solve for the pair correlation functions $g_{ab}(r)$ and the associated direct correlation functions $c_{ab}(r)$ are used to study these binary mixtures. For a mixture with n number of components, the OZ equation can be written and a $n \times n$ functional matrix equation:

$$\mathbf{SM} = \mathbf{I} \quad (23)$$

with $S_{ab} = S_{ab}(k)$ as defined by Eq.(16) and M_{ab} defined as

$$M_{ab}(k) = \delta_{ab} - \rho \sqrt{x_a x_b} \tilde{c}_{ab}(k) \quad (24)$$

where $\tilde{c}_{ab}(k)$ is the Fourier transforms direct correlation functions $c_{ab}(r)$.

In our case we consider binary mixtures with $n = 2$. hence we solve for the functions $g_{11}(r)$, $g_{12}(r)$ and $g_{22}(r)$, where 1 designates the first component

(the solvent) and 2 the second component (the solute). In the usual practice, these functions are discretized over an array of 2048 points, with a distance step of $\delta r = 0.02\sigma$. This allows to use fast Fourier transformation techniques to obtain the structure factors. We use a standard iterative technique to obtain the solutions of the 2 equations.

2.6 Computer simulations

We have used an in-house Monte Carlo code to perform Canonical ensemble simulations, with constant NVT. All simulations were made for an equimolar mixture of $N=4000$ particles. For each system, 50000 equilibration moves were initially done starting from a random mixture, and followed by 50000 sampling runs for statistical properties. This last step corresponds, in the usual formulation, to 200 millions Monte Carlo statistics per state points. The pair correlation functions obtained from such statistics are smooth enough to be directly compared with the corresponding quantities obtained from the IET techniques described above. We emphasize that the $g_{ab}(r)$ obtained in these simulations require a shift of their asymptote to the expected value 1, since it is now well known[7, 8] that finite size effects irremediably affect these asymptotes by a shift factor ϵ_{ab}/N , where N is the number of particle in the box and ϵ_{ab} is related to the concentration fluctuations within the box. We obtain the shifting factor empirically by enforcing the running integral $G_{ab}(r) = 4\pi \int_0^r u^2 du [g_{ab}^{(s)}(u) - 1]$ to reach a flat asymptote, where $g_{ab}^{(s)}(r) = g_{ab}(r)/(1 - \epsilon_{ab}/N)$ is the function corrected for the shift. Even though the functions obtained in this work tend to oscillate at long range due to domain correlations, the quantities $G_{ab}(r)$ usually tend to curve downward (for like correlations) or upward (for unlike correlation). This is corrected empirically through the factor ϵ_{ab} adjusted to straighten these asymptotes. For the type of models studied herein, in several cases, the shift was found to be negligibly small, and in such cases the procedure was ignored.

3 Results

The most important feature we would like to reproduce is the micro-segregation of the solvent and the solute, and the consequences of such micro-segregation on the structural properties, which are *i*) out-of-phase long range domain oscillations between like correlations $g_{11}(r)$, $g_{22}(r)$ and cross correlations $g_{12}(r)$, *ii*) subsequent domain pre-peaks in the structure factors $S_{ab}(k)$, which are positive for $S_{11}(k)$ and $S_{22}(k)$ and negative for $S_{12}(k)$. These latter signs are direct mathematical consequence of the fact that cross interaction leads

to depletion of species of opposite type, hence small short range correlations for $g_{12}(r)$ around the contact region. We wish to emphasize that correlation functions and structure factors of micro-structured systems have these features which are absent from the same quantities in simple liquids and mixtures. These features are essentially due to many body correlations, and approximate IET are not able to reproduce them, precisely because they lack contributions from such correlations.

Since the hypothesis behind Eq.(5) is to separate “frozen” many body correlations from random ones, it is important to appreciate the relative balance between these 2 terms. The guiding factor behind our investigation is the known fact, stated in the Introduction, that HNC is less accurate for core-softened models with an attractive part than with purely repulsive ones. The rationale behind this finding is that the second core tends to order particles around the central one by depleting their numbers, and the attractive component in the interaction tends to counter this depletion effect, leading to increase the probability of finding more particles around the central one, hence increasing the number of possibilities. Translated in terms of Eq.(5), the influence of attractive interactions is to increase the importance of $b_{ab}^{(RF)}(r)$, when we would prefer to reduce it, in order to appreciate the importance of $b_{ab}^{(LF)}(r)$.

In the next first two subsections we study previous categories of models, such as the SALR model or the non-additive model, both of which have been used to model micro-segregation. We demonstrate that none of these models allows to satisfactorily satisfy the hypothesis behind this work; namely to allows to fully neglect the random fluctuations contributions from many body correlations.

3.1 Unsuccessful model: the Y-SRLA

A first natural idea was to follow the SALR pathway and use Yukawa interactions for $v_{12}^{(\text{rep})}(r)$ and $v_{12}^{(\text{att})}(r)$ in Eq.(21) The resulting model we named Y-SRLA (with the Y for Yukawa), leading to

$$v_0(r) = v_{12}^{(0)}(r) = 4\epsilon_0 \left(\frac{\sigma}{r}\right)^{12} \quad (25)$$

$$v_{12}^{(\text{rep})}(r) = \epsilon_1 \sigma \frac{\exp[-(r - \sigma)/\kappa_1]}{r} \quad (26)$$

$$v_{12}^{(\text{att})}(r) = -\epsilon_2 \sigma \frac{\exp[-(r - \sigma)/\kappa_2]}{r} \quad (27)$$

It turned out that this model could not produce satisfactory domain segregation, such as to produce wide oscillatory domain correlations in the long range. In addition the agreement between theory and simulation was quite weak, and specially more so when we tried to increase the domain correlations. The reason for this problem can be tracked to an important feature of this Yukawa interaction, which lead us to a change in strategy. The problem is the existence of the range parameters κ_i , which in fact introduce an additional length scale into the problem, in addition to the slow exponential decay. It turns out that what seems required for domain oscillation is not a range+decay, but a *localisation* of the interaction. We found this out by substituting a Gaussian to the second exponential. We believe that this is an important information concerning the nature of the frozen many body correlations. They cannot be properly modeled by screened Coulomb interactions which do not localize the particles very well. In particular, it would seem that the second attractive interaction requires to be localized such as a Gaussian.

3.2 Unsuccessful model: the non-additive SRLA

With the failure of the previous model, we turned our attention to non-additive interactions (hence the name NA-SRLA). However, since non-additivity is more toy model than one suited to describe realistic systems, we have tested models where is the cross interaction dispersive interaction range which controls the long range re-mixing. In this context, the non-additivity is brought by the short range repulsion $\tilde{v}_{12}^{(\text{rep})}(r)$. The interaction considered in this section are of the form:

$$v_0(r) = 4\epsilon_0 \left[\left(\frac{\sigma}{r} \right)^{12} - \lambda_0 \left(\frac{\sigma}{r} \right)^6 \right] \quad (28)$$

and the generic form for the cross interaction becomes:

$$\tilde{v}_{12}(r) = 4\epsilon_{12} \left[\left(\frac{\sigma_{12}}{r} \right)^{12} - \lambda \left(\frac{\sigma_{12}}{r} \right)^6 \right] + \epsilon_2 \exp \left[-(r - \alpha_1)^2 / \kappa_1^2 \right] \quad (29)$$

With this form, the extension of the repulsive part covers both first terms in Eq.(21)

Fig.1(a-b) shows one such typical trial for the following parameters, $\epsilon_0 = 1$, $\lambda_0 = 1$, $\epsilon_{12} = 2.8$, $\lambda = 1$, $\epsilon_1 = 40$, $\alpha_1 = 0.75$, $\kappa_1 = 0.2582$, and for state parameters temperature $T = 1$ and packing fraction $\eta = (\pi/6)\rho = 0.4$. The pair interactions shown in the inset of Fig.1a shows how the repulsive part

of the cross interaction installs a pseudo non-additivity, while at the same time allowing for a long range attraction through the depth controlled by the large value of ϵ_{12} .

In this figure, we can see that the domain oscillations do not develop very well, although the corresponding positive and negative pre-peaks at $k\sigma_1 \approx 2$ are quite apparent in Fig.1b. In addition, the agreement with simulation remains qualitative, much like the one found for the Y-SRLA model mentioned in the previous section. The BT structure factors shown in the lower inset of Fig.1b indicate that the $S_{NN}(k)$ looks very much as a 1-component structure factor of ordinary LJ liquid, while the $S_{CC}(k)$ shows a prominent pre-peak corresponding to those of $S_{11}(k)$ and $S_{22}(k)$, hence witness the clustering induced heterogeneity in the system, as expected from the input pair interaction. This inset provides a direct illustration of the separation, mentioned in Section 2.1, of the homogeneous and heterogeneous components of the $S_{ab}(k)$ structure factors, into $S_{NN}(k)$ and $S_{CC}(k)$, respectively. It also shows that while the former is well reproduced by HNC, it is quite inaccurate in the latter, as shown by the larger pre-peak HNC predicts.

In a second example in Fig.2(a-b), we considered purely repulsive first term, in order to get rid of the fluctuations associated to the short range attraction in the like interaction part, with the expectation to get a better agreement between simulations and IET. Fig.2(a-b) illustrate the results with parameters $\epsilon_0 = 1$, $\lambda_0 = 0$, $\epsilon_{12} = 1$, $\lambda = 1$, $\epsilon_1 = 4$, $\alpha_1 = 0.85$, $\kappa_1 = 0.4663$, and for state parameters temperature $T = 1$ and packing fraction $\eta = (\pi/6)\rho = 0.4$

One important drawback of this model is that it was impossible to get into the regime where the $k = 0$ values were large, with smaller pre-peaks, that were in good agreement with simulations. This is crucial to describe near-demixing situations, where the cross LJ attraction is too small compared to the short range repulsion which guides the demixing. It would seem that, when we neared such conditions, the differences between the (exact) simulation results and the theory started to differ. This situation reminds what happens in simple liquids near demixing transitions, where the contribution of fluctuations do not allow the theory to work well. We traced back this situation to the fact of keeping a LJ interaction for the first part, a form which is reminiscent of the simple liquids, for which the theory is not so good. The upper inset of Fig.2b, as well as the BT structure factors in the lower inset show that HNC overestimates the heterogeneity in the $S_{CC}(k)$ pre-peak as compared with simulations.

From the perspective of the conjecture formulated herein, the form of the pseudo-potential proposed in Eq.(29) seems to leave a rather large part of the many body correlation description into the $b^{(R)}(r)$ part mentioned

in Eq.(5), as witnessed by the inappropriate reproduction of the pre-peak feature. Hence, it makes this form not suitable for proper modeling of the heterogeneity bridge function.

3.3 Successful model: the G-SRLA

In the final form, we settled for using Gaussian for both terms $v_{12}^{(\text{rep})}(r)$ and $v_{12}^{(\text{att})}(r)$, which turned out to be the correct choice. It confirms the hints provided in sub-section 3.1, where the localisation seems to be the keyword. The exact forms of the interactions used for this study are:

$$v_{11}(r) = v_{22}(r) = 4\epsilon_0 \left(\frac{\sigma_{12}}{r} \right)^{12} \quad (30)$$

$$\tilde{v}_{12}(r) = 4\epsilon_{12} \left(\frac{\sigma}{r} \right)^{12} + \epsilon_1 \exp \left[-(r - \alpha_1)^2 / \kappa_1^2 \right] - \epsilon_2 \exp \left[-(r - \alpha_2)^2 / \kappa_2^2 \right] \quad (31)$$

with generic parameters $\epsilon_0 = \epsilon_{12} = 1$, and for state parameter temperature $T = 3$ and packing fraction $\eta = (\pi/6)\rho = 0.4$. The parameters of the first Gaussian have been fixed at $\epsilon_1 = 0.5$, $\alpha_1 = 1.5$, $\kappa_1 = 0.41$, and for the second Gaussian, we fixed the parameters $\alpha_2 = 3$, $\kappa_2 = 0.41$ and varies the depth ϵ_2 of the attraction to describe various cases. It is this depth which controls the segregation. In the following figures, we illustrate how this form allows to describe the 3 typical situations, ranging from near demixing to full domain segregation, particularly visible in the shape of the structure factors in the small-k region.

Fig.3(a-b) show the near demixing, with large $k = 0$ values for the structure factors. Demixing is enhanced when $\epsilon_2 = 0$, since there are only repulsive cross interactions. We start with a small ϵ_2 parameter, namely $\epsilon_2 = 0.015$, in order to see how much it helps re-entrant mixing. It is seen that this is yet not similar to the usual demixing in simple liquids, since the cross term is negative. It is seen that, although the agreement between the calculated and simulated correlations are in close agreement in the short to medium range part, there is a small difference in the long range part, which leads to structure factors that differ quite strongly near $k = 0$. This is probably due to the hidden influence of the random fluctuation part $b^{(RF)}(r)$, which we totally neglect in the HNC theory. This disagreement reveals that we cannot expect the HNC theory to describe properly systems close to true phase transitions, for the lack of knowing how critical fluctuations influence correlations. Nevertheless, the agreement is much better than in the 2 previous cases. The BT structure factors in Fig.3b show that the small-k raise is not due to critical

fluctuation, in which case it would appear in $S_{NN}(k)$, but to the heterogeneity, since it appears in $S_{CC}(k)$. This is an interesting demonstration that large heterogeneity can be mistaken for critical concentration fluctuation, and that the BT transformation can help figure out such cases. On the other hand, it is clear that, when $\epsilon_2 \rightarrow 0$ in Eq.(31) then true critical demixing will occur because of the purely repulsive cross interactions. Hence, Fig.3(a-b) appears as a show case for many realistic aqueous mixtures, such as water-acetonitrile for example, which show both considerable heterogeneity and demixing-like behaviour[9, 10].

Fig.4(a-b) shows an intermediate case, for the parameter $\epsilon_2 = 0.030$, which corresponds to increasing the depth of the attractive interaction with respect to the previous case in Fig.3. This is a very interesting case from physical point of view, since it concerns a system which hesitates between demixing and micro-segregation. This is usually called a Lifshitz point[11], and our model is capable of describing this physical situation in excellent agreement with simulations. The Lifshitz point appears in many circumstances in the context of micro-emulsions, where there is a triple coexistence between two homogeneous and a layered phase[5, 11]. But, in the present case, it describes the turning point between segregated phase and a micro-segregated phase. Such phase was found in a realistic mixture of water and diols in a previous study.

Fig.5(a-b) illustrates the case with full micro-segregation and domain ordering. It corresponds to the parameter $\epsilon_2 = 0.12$. We note the quasi perfect agreement between HNC and simulations both in the correlation and structure factors, particularly for the BT ones.

Finally, Fig.6(a-b) described a case where we vary the Gaussian width parameter in order to increase the region of micro-segregation. It corresponds to parameters $\epsilon_2 = 0.025$ but we also modify $\kappa_2 = 4.47$. This particular example shows very clearly how domain oscillations appear in conjunction with a growth of the pre-peaks in the structure factors witnessing domain-domain correlations. These features look very similar to those we have reported in several types of aqueous mixtures[30, 31]. Similar results are equally obtained when ϵ_2 is kept fixed while varying κ_2 . This shows that the model is very flexible, in terms both height and width of the second Gaussian, and more importantly allows to control the extinction of the second bridge term $b_{ab}^{RF}(r)$, thus making HNC an exact relation in terms of the effective interaction.

From the results above, we propose that the cross bridge term for real clustering and micro-segregated system may be efficiently modeled as a sum of two Gaussians:

$$b_{12}^{(LF)}(r) = -\beta\epsilon_1 \exp \left[-(r - \alpha_1)^2 / \kappa_1^2 \right] + \beta\epsilon_2 \exp \left[-(r - \alpha_2)^2 / \kappa_2^2 \right] \quad (32)$$

The application of the above expression for realistic systems remains to be tested for various cases. We expect that the insertion of the above expression in the pair correlation function between the principal hydrogen bonding atoms of different species will take into account the main feature of the micro-segregation, and allow HNC to be finally solve for such systems.

4 Discussion

In order to formulate the existence of the separation in Eq.(5) we have implicitly accepted the existence of domain correlations in complex liquids, in particular aqueous mixtures, and more importantly that such domains emerge a new form of interaction, which can be captured through the bridge terms $b^{(LF)}(r)$, the lack of which will not permit to find numerical solution with the HNC IET. Insights into such correlations are obtained from our own previous investigations into these systems. Long range domain oscillations were observed from computer simulations of aqueous-1propanol[31] and also ethanol-benzene mixtures[8]. These oscillations simply reflect the local segregation into nano-domains of each species.

In view of the fact that previous models such as SALR models have been designed to mimic aggregates in pseudo-one component systems, our approach provides a link between the domain segregation observed in complex mixtures and the models such as SALR models. In Section 2.2 we have demonstrated that such effective models which capture the complexity of the disorder (clustering, self-segregation, and others), are in fact formulating explicit expressions for the many body correlation bridge terms, in particular those related to local fluctuations $b_{ab}^{(LF)}(r)$. In section 3, we have used this property of effective models to provide explicit expressions for the cross species bridge term $b_{12}^{(LF)}(r)$.

The study provided in Section 3.3 clearly indicates that the $k = 0$ raise in the structure factor cannot be solely attributed to random fluctuations such as those appearing near spinodal lines or critical points. This is a very important point, and a hint to this problem has been previously provided in the study of such system in the two-dimensional cases[12].

The previous point does not exclude the fact that the $k = 0$ raise observed for simple liquids in the vicinity of mechanical instability remains of point delicate to investigate through the IET methodology. This means that systems which tend to organise locally and which are submitted to large random

fluctuations, will not be well described by the methodology employed here. Indeed, in both such cases, the form of the $b_{ab}^{(RF)}(r)$ is important, and this term cannot obviously be neglected. We have no clue as to how to address situation where random fluctuations are important part of the physics of the system, and this remains an important subject for investigations in the IET methodology.

The separation of the many body correlations into contributions from frozen fluctuations and those random fluctuations should generally allow to reproduce the correlations complex soft-matter systems. For example, micro-emulsions, with the formation of micelles is a first target for extending IET techniques into soft matter liquids.

5 Conclusion

The results shown herein demonstrate that one could extend the HNC IET in a reliable way deep into the strongly micro-heterogeneous mixtures. This is accomplished by taking into account specific correlations which produce this micro-heterogeneity directly into the pair-interaction. In this work, we have explicitly designed simplified systems, which incorporate directly into the pair interactions the features which produce the micro-heterogeneity, which is why we could solve the IET for such systems. The search for such simplified models indicate that taking into account the fluctuations which produce the heterogeneity gives important insights into the nature of the underlying many body correlations. The division into frozen and fluctuating contribution, allows to both test the accuracy of the HNC closure, and also appreciate the role of fluctuations in this closure. The extension of this methodology to realistic mixtures is the next step. Although the approach remains empirical, we expect that some general schemes would emerge, in particular for mixtures involving hydrogen bonding molecules. While the principal challenge remains to capture the frozen fluctuations which produce the micro-heterogeneity, the role of the random fluctuations would assess the reliability of the IET and the HNC approximation. Our expectation is that, far from phase transition, this methodology should produce good results since random part of fluctuations are supposed to be small. In any case, this approach will certainly help to appreciate the relative importance of both these types of many body correlations.

Acknowledgments

A. B. thanks Laboratoire de Physique Théorique de la Matière Condensée for his first year Master internship.

References

- [1] J. E. Mayer and M. G. Mayer, *Statistical Mechanics* (Wiley, New York, 1940)
- [2] R. J. Baxter, *Exactly Solved Models in Statistical Mechanics*, Academic Press (London 1982)
- [3] J.P. Hansen and I.R. McDonald, *Theory of Simple Liquids* (Academic, London, 1986)
- [4] C. Caccamo, Phys. Rep. **274**, 1 (1996)
- [5] A. Parola and L. Reatto, *Advances in Physics* **44**, 211 (1995)
- [6] G. Sarkisov and E. Lomba, J. Chem. Phys **122**, 214504 (2005)
- [7] A. Perera and B. Kežić, *Faraday Discuss.* **167**, 145 (2013)
- [8] A. Perera and B. Lovrinčević, *Molecular Physics* **116**, 3311 (2018)
- [9] T. Morita and K. Hiroike, *Prog. Theor. Phys (Japan)*, **23**, 1003 (1960)
- [10] W. G. Hoover and A. G. de Rocco, J. Chem. Phys. **36**, 3141 (1962)
- [11] A. Perera, *Mol. Phys.* **107**, 2251 (2009)
- [12] L. Lue and D. Blankschtein, J. Phys. Chem. **96**, 8582 (1992)
- [13] M. Munafo, D. Costa, F. Saija and C. Caccamo, J. Chem. Phys. **132**, 084506 (2010)
- [14] L. Verlet, *Phys. Rev.* **163**, 201 (1968)
- [15] F. J. Rogers and D. A. Young, *Phys. Rev.* **E30**, 999 (1984)
- [16] G. Zerah and J. P. Hansen, J. Chem. Phys. **84**, 2336 (1986)
- [17] S. Labík, H. Gabrielová, J. Kolafa and A. Malijevsky, *Mol. Phys.* **101**, 1139 (2003)

- [18] M. Baus and J.-P. Hansen, Physics Reports **59**, 1 (1980)
- [19] Y. Wang and G; A. Voth, J. Am. Chem. Soc. **127** 12192 (2005)
- [20] A. Perera and R. Mazighi, J. Mol. Liq. **210**, 243 (2015)
- [21] A. Perera , Phys. Chem. Chem. Phys. **19**, 1062 (2017)
- [22] K.-C. Ng, J. Chem. Phys. **61** , 2681 (1974)
- [23] G. Malescio and Pellicane, Nat. Mater. **2**, 97 (2003).
- [24] E. A. Yagla, Phys. Rev. **E58**, 1478 (1998)
- [25] G. Franzese, G. Malescio, A. Skibinsky, S. V. Buldyrev and H. E. Stanley, *Nature* **409**, 692 (2001)
- [26] A. Perera, Mol. Phys. **107**, 487 (2009).
- [27] A. Perera, A. Rispe L. Zoranić, R. Mazighi and F. Sokolić, Mol. Phys. **107**, 1349 (2009)
- [28] S. Dixit, J. Crain, W. C. Poon, J. L. Finney and A. K. Soper, *Nature* **416**, 829 (2002)
- [29] S. Weerasinghe and P. E. Smith, J. Chem. Phys. **118**, 10663 (2003)
- [30] A. Perera, Pure and Appl. Chem. **88** ,189 (2016)
- [31] A. Perera Phys. Chem. Chem. Phys. **19**, 28275 (2017)
- [32] J. L. Barrat, J. P. Hansen and G. Pastore, Mol. Phys. **63**, 747 (1988)
- [33] D. Levesque and J. J. Weis, Phys. Rev. E **49**, 5131 (1994)
- [34] D. Chandler and H. C. Andersen, J. Chem. Phys. **57** , 1930 (1972)

References

- [1] L. Lue and D. Blankstein, J. Chem. Phys. **102** , 5427 (1995)
- [2] J. Bomont, J. Bretonnet, D. Costa, and J. Hansen, J. Chem. Phys. **137**, 011101 (2012).
- [3] P. Godfrin, R. Castañeda-Priego, Y. Liu, and N. Wagner, J. Chem. Phys. **139**, 154904 (2013).

- [4] F. Sciortino, S. Mossa, E. Zaccarelli, and P. Tartaglia, Phys. Rev. Lett. **93**, 055701 (2004).
- [5] A. J. Archer and N. B. Wilding, Phys. Rev. E **76**, 031501 (2007)
- [6] A. B. Bhatia and D. E. Thornton, Phys. Rev. **B 2**, 3004 (1970)
- [7] J.L. Lebowitz, J.K. Percus, Phys. Rev. **122** (1961) 1675.
- [8] M. Požar et al. Physical Chemistry Chemical Physics, **17**, 9885 (2015)
- [9] K. Nishikawa, Y. Kasahara and T. Ichioka, J. Phys. Chem. **B 106**, 693 (2002)
- [10] R. D. Mountain, J. Phys. Chem. **A 103**, 10744 (1999)
- [11] A. Ciach, Phys. Rev. E **78**, 061505 (2008)
- [12] A. Perera and T. Urbic , Physica A **495**, 393 (2018)

Figure captions

- Fig.1 Pair correlation functions (a) and corresponding structure factors (b) for the model NA-SRLA, for parameters $\epsilon_0 = 1$, $\lambda_0 = 1$, $\epsilon_{12} = 2.8$, $\lambda = 1$, $\epsilon_1 = 40$, $\alpha_1 = 0.75$, $\kappa_1 = 0.2582$, and for a temperature of $T = 1$ and packing fraction $\eta = 0.4$. HNC results in full lines (blue for 11 component pair and dark green for 12) and simulation in dashed (cyan for 11 component pair and green for 12). The inset in (a) represents the effective pair interactions with full lines for 11 (blue) and 12 (red) and the details for 12 are shown in dotted lines (LJ part in magenta and Gaussian part in cyan). The inset in (b) represents the BT structure factors (HNC results for $S_{NN}(k)$ and $S_{CC}(k)$ in full blue and dark green lines, respectively, simulations results in dashed cyan and green lines, respectively)
- Fig.2 Same as Fig.1, but the repulsive interaction for 11 components and for parameters $\epsilon_0 = 1$, $\lambda_0 = 0$, $\epsilon_{12} = 1$, $\lambda = 1$, $\epsilon_1 = 4$, $\alpha_1 = 0.85$, $\kappa_1 = 0.4663$ and same state parameters as in Fig.1. (upper inset in (b) is a zoom on the pre-peak area).
- Fig.3 Pair correlation functions (a) and corresponding structure factors (b) for the model G-SRLA, for parameters $\epsilon_0 = \epsilon_{12} = 1$, $\epsilon_1 = 0.5$, $\alpha_1 = 1.5$, $\kappa_1 = 0.41$, $\alpha_2 = 3$, $\kappa_2 = 0.41$. The lines and color codes are as in Fig.1
- Fig.4 Pair correlation functions (a) and corresponding structure factors (b) for the model G-SRLA, for the same interaction parameters as in Fig.3, except for $\epsilon_2 = 0.030$. The lines and color codes are as in Fig.1
- Fig.5 Pair correlation functions (a) and corresponding structure factors (b) for the model G-SRLA, for the same interaction parameters as in Fig.3, except for $\epsilon_2 = 0.12$. The lines and color codes are as in Fig.1
- Fig.6 Pair correlation functions (a) and corresponding structure factors (b) for the model G-SRLA, for for the same interaction parameters as in Fig.3, except for $\epsilon_2 = 0.025$ and $\kappa_2 = 4.47$. The lines and color codes are as in Fig.1. (upper inset in (b) is a zoom on the pre-peak area).

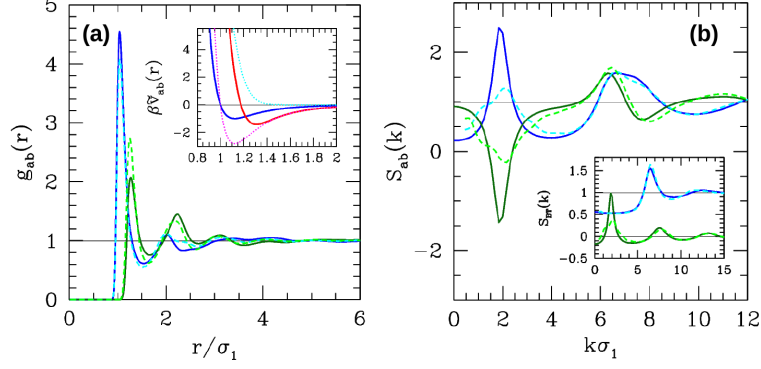


Fig.1 - Pair correlation functions (a) and corresponding structure factors (b) for the model NA-SRLA, for parameters $\epsilon_0 = 1$, $\lambda_0 = 1$, $\epsilon_{12} = 2.8$, $\lambda = 1$, $\epsilon_1 = 40$, $\alpha_1 = 0.75$, $\kappa_1 = 0.2582$, and for a temperature of $T = 1$ and packing fraction $\eta = 0.4$. HNC results in full lines (blue for 11 component pair and dark green for 12) and simulation in dashed (cyan for 11 component pair and green for 12). The inset in (a) represents the effective pair interactions with full lines for 11 (blue) and 12 (red) and the details for 12 are shown in dotted lines (LJ part in magenta and Gaussian part in cyan). The inset in (b) represents the BT structure factors (HNC results for $S_{NN}(k)$ and $S_{CC}(k)$ in full blue and dark green lines, respectively, simulations results in dashed cyan and green lines, respectively)

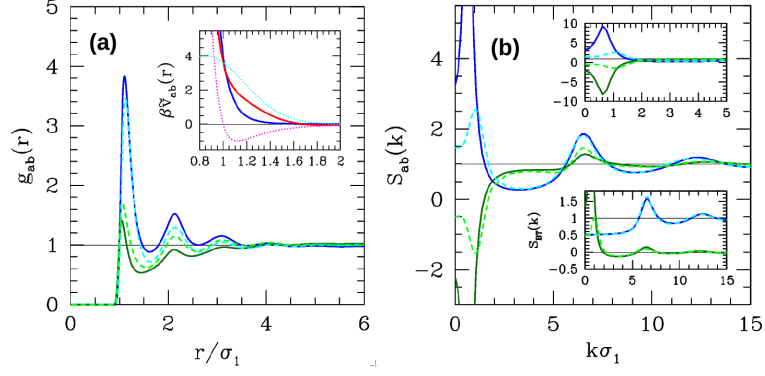


Fig.2 - Same as Fig.1, but the repulsive interaction for 11 components and for parameters $\epsilon_0 = 1$, $\lambda_0 = 0$, $\epsilon_{12} = 1$, $\lambda = 1$, $\epsilon_1 = 4$, $\alpha_1 = 0.85$, $\kappa_1 = 0.4663$ and same state parameters as in Fig.1. (upper inset in (b) is a zoom on the pre-peak area)

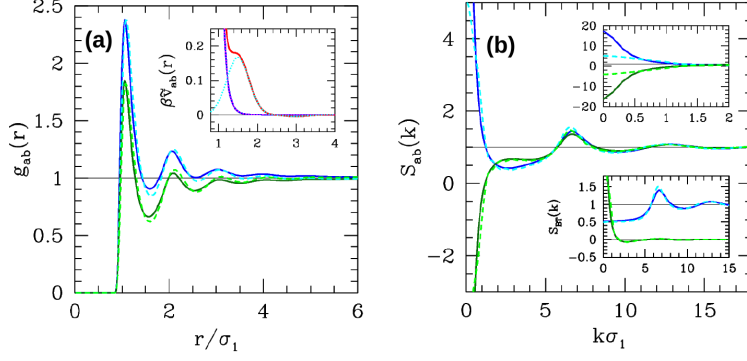


Fig.3 - Pair correlation functions (a) and corresponding structure factors (b) for the model G-SRLA, for parameters $\epsilon_0 = \epsilon_{12} = 1$, $\epsilon_1 = 0.5$, $\alpha_1 = 1.5$, $\kappa_1 = 0.41, \alpha_2 = 3$, $\kappa_2 = 0.41$. The lines and color codes are as in Fig.1

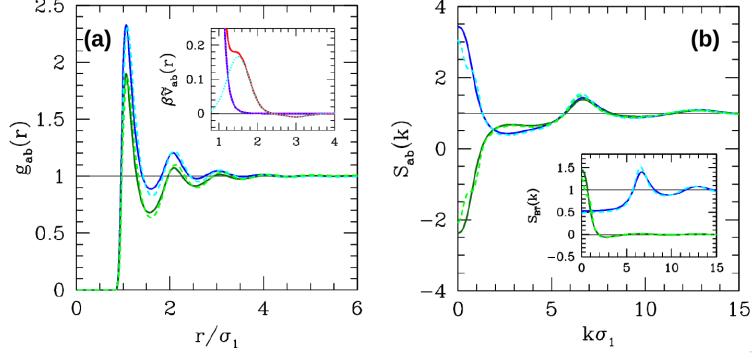


Fig.4 - Pair correlation functions (a) and corresponding structure factors (b) for the model G-SRLA, for the same interaction parameters as in Fig.3, except for $\epsilon_2 = 0.030$. The lines and color codes are as in Fig.1

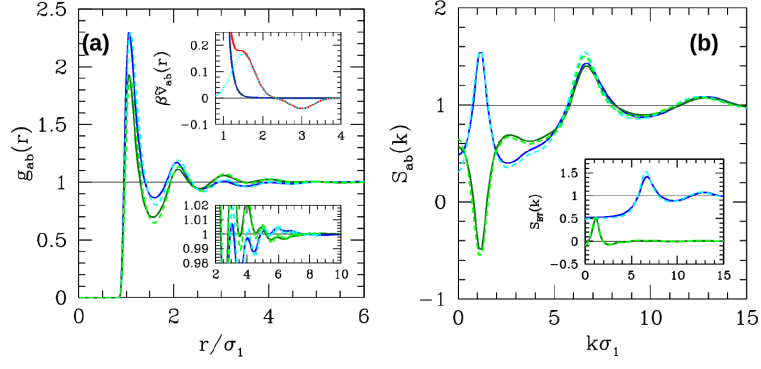


Fig.5 - Pair correlation functions (a) and corresponding structure factors (b) for the model G-SRLA, for the same interaction parameters as in Fig.3, except for $\epsilon_2 = 0.12$. The lines and color codes are as in Fig.1

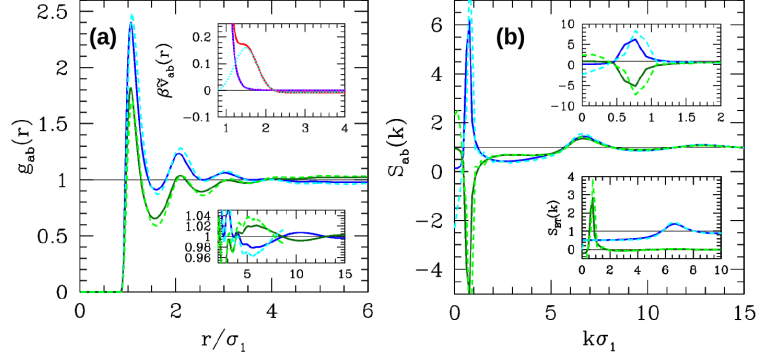


Fig.6 - Pair correlation functions (a) and corresponding structure factors (b) for the model G-SRLA, for the (upper inset in (b) is a zoom on the pre-peak area) same interaction parameters as in Fig.3, except for $\epsilon_2 = 0.025$ and $\kappa_2 = 4.47$. The lines and color codes are as in Fig.1.